Magnetic and conductive dead layer at the $La_{0.67}Ca_{0.33}MnO_3$–$SrTiO_3$:Nb interface

S. Liang, J. R. Sun,[a] J. Wang, and B. G. Shen
Beijing National Laboratory for Condensed Matter Physics and Institute of Physics, Chinese Academy of Sciences, Beijing 100190, People's Republic of China

(Received 18 August 2009; accepted 20 October 2009; published online 6 November 2009)

Interfacial properties of the $La_{0.67}Ca_{0.33}MnO_3$ films grown on $SrTiO_3$ and $SrTiO_3$:Nb, respectively, have been experimentally studied. An interface layer, ~13 or ~4.4 nm for the films on $SrTiO_3$ or $SrTiO_3$:Nb, with degenerated magnetic/conductive properties is found in the film. The most remarkable result is the significantly different layer width on different substrates. The built-in electric field yielded by charge exchange may be responsible for the layer shrinkage in $La_{0.67}Ca_{0.33}MnO_3/SrTiO_3$:Nb. A depression of this layer by magnetic field is also observed and ascribed to field-induced enhancement of the double exchange between Mn ions. © *2009 American Institute of Physics*. [doi:10.1063/1.3262951]

In general, the surface/interface properties of the materials are different from those of the bulk. They are particularly important in the cases when interfacial processes are invoked, such as interlayer transport and interlayer coupling that dominates the properties of the multilayer/superlattice-structured materials. Manganites are the focus of the past decade because of their magnetic-transport coupling that leads to a colossal magnetoresistance. The first report on the magnetic degeneration of the surface layer in manganite films was given by Park *et al.*[1] Subsequent studies conducted by Sun *et al.*[2] declared the presence of a magnetic/conductive dead layer at the manganite-substrate interface. The occurrence of phase separation, due to lattice distortions and related structural defects, was then proposed to be responsible for the degeneration of the interfacial property.[3] The interface layer was further found to be susceptible to external stimuli, and a recent research revealed a dramatic enhancement of the interface conduction.[4]

The interface layer may strongly depend on substrate, especially when charge exchange exists between the film and the substrate, as occurred in the manganite/$SrTiO_3$:Nb heterojunctions.[5] As well established, manganite is hole-doped in character whereas $SrTiO_3$:Nb is electron-doped, and there is a mutual hole/electron diffusion between the two oxides.[6] In this case, the information on the magnetic/conductive state of the interface layer is particularly valuable, it may lead to a deep insight into the physics underlying the diverse behaviors of the junctions. However, whether a dead layer exists, its thickness and variation under magnetic field, which are important issues that have to be considered by the manganite engineering, have been scarcely addressed before. In this letter, we will perform a systematic study on the conductive and magnetic properties of the $La_{0.67}Ca_{0.33}MnO_3$ films grown on $SrTiO_3$ and $SrTiO_3$:Nb, respectively. An interface layer with degenerated magnetic and conductive properties has been observed. It is fascinating that this layer is much thinner in the films on $SrTiO_3$:Nb than on $SrTiO_3$ and considerably shrinks in width under magnetic field.

Two series of samples were fabricated by growing, using the pulsed laser ablation technique, $La_{0.67}Ca_{0.33}MnO_3$ (LCMO) films on the (001)-$SrTiO_3$ (STO) and the 0.05 wt % Nb-doped $SrTiO_3$ (STON) substrates, respectively. During the deposition, the sample holder, on which the STO and STON substrates were mounted side by side, was kept at 720 °C and the oxygen pressure at 80 Pa. The sample size is 1.5×5 mm^2, and the film thickness is $t=7$, 16, 25, 34, and 45 nm, controlled by deposition time. The resultant samples were analyzed by x-ray diffraction (XRD) and atomic force microscope (AFM). Magnetic and resistive measurements were performed by a superconducting quantum interference device magnetometer equipped by a resistance measurement unit.

As reported, the LCMO films are clean single phase and epitaxially grown. Figure 1(a) exemplifies the XRD pattern recorded around the (002) peak (indexed based on the cubic perovskite structure) of the LCMO/STON film of 35 nm. As a consequence of lattice relaxation, the out-of-plane lattice constant shows a gradual growth with the increase of film thickness. Essentially the same lattice parameters are observed for the two series of samples. The rocking curve of the (002) peak is also measured. The full width at half height is ~0.2° for the LCMO/STO films and ~0.32° for the LCMO/STON films, without obvious dependence on film thickness. The crystal orientation of the LCMO films is fairly

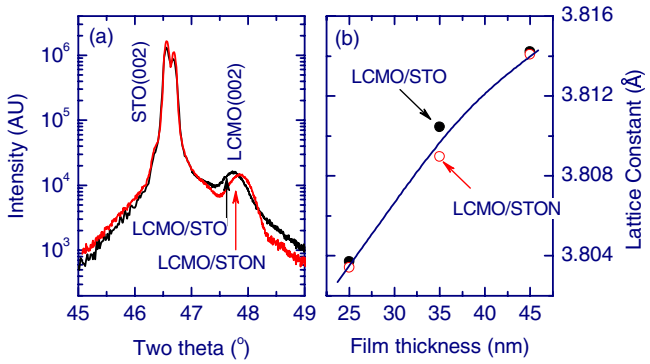

FIG. 1. (Color online) (a) XRD pattern of the LCMO films of 35 nm, recorded around the (002) peak. (b) Lattice constant as a function of film thickness. Solid lines are guides for the eyes.

[a]Author to whom correspondence should be addressed. Electronic mail: jrsun@g203.iphy.ac.cn.

 © 2009 American Institute of Physics

Author complimentary copy. Redistribution subject to AIP license or copyright, see http://apl.aip.org/apl/copyright.jsp

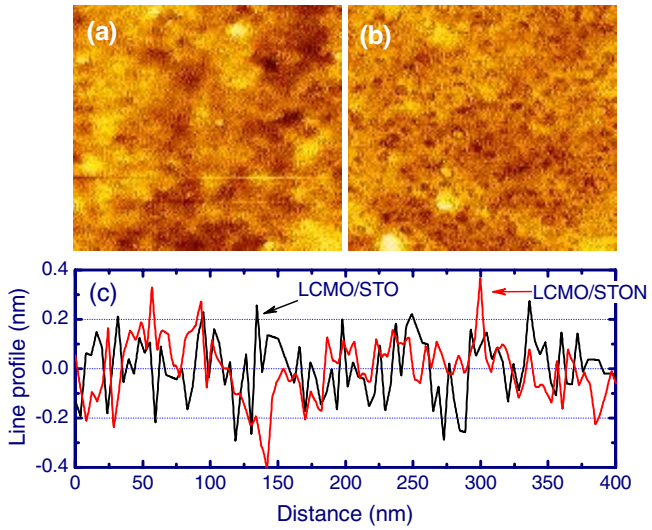

FIG. 2. (Color online) AFM images of the LCMO/STON (a) and LCMO/STO (b) films of 45 nm (1×1 μm^2), obtained by AFM. (c) Typical line profiles of the surface morphology of the LCMO films.

good compared with the single crystal substrate (~0.14°), though it is different for LCMO/STO and LCMO/STON.

The films are quite smooth, as revealed by the AFM analysis. The root-mean-square roughness of the films varies between 0.2 and 0.6 nm, without systematic difference for the two series of films. Figures 2(a)–2(c) present the typical AFM images and line profiles of the LCMO films (45 nm). The peak-to-valley fluctuation is generally below ~0.4 nm, the height of an unit cell.

Figures 3(a) and 3(b) show the resistivity (ρ) of the LCMO films, measured by the standard four-probe technique

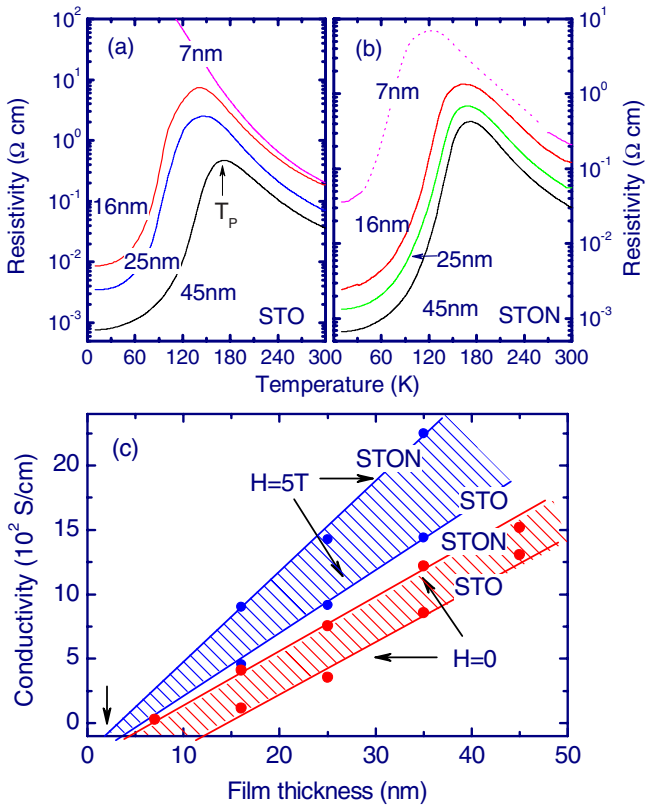

FIG. 3. (Color online) Temperature dependence of the resistivity of the LCMO films on the STO (a) and STON (b) substrates. (c) Conductivity as a function of film thickness. Solid and dotted lines are guides for the eyes.

along the LCMO plane with an applied current of 1 μA. The resistance of the LCMO films was also measured under a constant current of 0.1 μA, and no visible difference is observed. For the films thicker than 7 nm, the bypass effect of the STON substrate is negligible because of the extremely high resistance across the LCMO-STON interface, the latter is generally greater than $\sim10^7$ Ω at the room temperature and grows rapidly upon cooling. The in-plane resistance of LCMO(7 nm)/STON is comparable to that of the junction, and only the data above 260 and below 40 K are reliably measured. The maximum resistance is $\sim1.5\times10^4$ Ω at 5 K, occurring in the LMCO film of 7 nm, which is much lower than the junction resistance. As shown by Fig. 3, with the decrease of temperature, the resistivity of the film undergoes first an exponential growth, above a character temperature T_P, then a rapid decrease, which is the typical behavior of the LCMO films. With the decrease of film thickness, an increase in resistivity and an accompanied decrease in T_P appear. Compared with LCMO/STO, films on STON show a slower increase in resistivity upon thickness reduction. This is especially obvious in the films of 7 nm: A signature of insulator-metal transition can still be recognized in LCMO(7nm)/STON, whereas LCMO(7 nm)/STO keeps insulating down to 5 K. As film thickness reduces from 45 to 16 nm, the residual resistivity $\rho(0)$, obtained by extrapolating the $\rho(T)$ curve to $T=0$, grows from $\sim7.65\times10^{-4}$ to $\sim5.58\times10^{-3}$ Ω cm for the LCMO/STO films, with a totally growth of $\Delta\rho/\rho\approx629\%$. In contrast, the corresponding change in the LCMO/STON films is from $\sim6.68\times10^{-4}$ to $\sim2.45\times10^{-3}$ Ω cm ($\Delta\rho/\rho\approx267\%$).

As proven by Sun *et al.*,[2] the increase of resistivity with decreasing film thickness indicates the presence of a dead layer with reduced conductivity. As shown by Fig. 3(c), the conductivity exhibits a linear reduction with the decrease of film thickness. By extrapolating the σ-t relation to $\sigma\rightarrow0$ ($\sigma=1/\rho$), we obtain the effective thickness of the conductive dead layer, and it is $\sim6.5\pm0.6$ nm for the LCMO/STON film and $\sim14.6\pm3.1$ nm for the LCMO/STO film. The $\rho(T)$ relation of the LCMO films is also studied in the presence of a field of 5 T (results not shown), and similar analysis gives the dead layer thickness of $\sim3.8\pm2.2$ nm for LCMO/STON and $\sim7.3\pm1.0$ nm for LCMO/STO. The decrease of the dead layer width under magnetic field is understandable. Magnetic field can stabilize the ferromagnetic or the conductive state by improving the double exchange between Mn ions. Compared with LCMO/STO, changes in the dead layer in LCMO/STON are obviously small. This result reveals the robustness of the insulting state near the interface, and explains the absence of strong effect of magnetic field on manganite junctions.[7]

To get the information on the evolution of the magnetic order with film thickness, the magnetization (M) of the LCMO films is further studied. As a representative, Fig. 4(a) presents the thermomagnetization curves of the LCMO films of 35 nm, measured under a field of 0.05 T in the zero-field cooled mode. With the decrease of temperature, a paramagnetic-to-ferromagnetic transition, marked by a rapid growth of the magnetization, can be clearly seen. With the decrease of film thickness, there is no obvious broadening in transition width except for the film of 7 nm. The Curie temperature, defined by the inflection points in the $M(T)$ curve, displays first a smooth then a fast decrease with the decrease

Author complimentary copy. Redistribution subject to AIP license or copyright, see http://apl.aip.org/apl/copyright.jsp

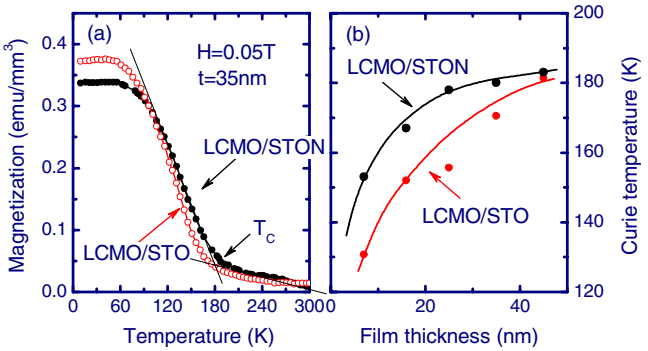

FIG. 4. (Color online) (a) Temperature dependence of the magnetization of the LCMO films of 35 nm, measured in a field of 0.05 T. (b) Curie temperature as a function of film thickness. Straight lines in the figure denote the definition of the Curie temperature. Solid lines are guides for the eyes.

of film thickness. The largest change of T_c takes place as t changes from 16 nm to 7nm, occurring in both series of films [Fig. 4(b)]. Correspondingly, the magnetization experiences a sudden drop. Noting that 7 nm is near or lower than the widths of the dead layer, these results imply a weakening of the magnetic coupling in the insulating layer. There is an exact correspondence between the T_c reduction and the $\rho(0)$ growth (Figs. 3 and 4). This is plausible since the decrease of T_c indicates the weakening of the double exchange. Similar tendency is observed in the T_P-t relation (not shown here).

The most remarkable result of the present study is that the dead layer in LCMO/STON is thinner than that in LCMO/STO. As well known, the charge carrier is holelike in LCMO while electronlike in STON. Mutual carrier diffusion between LCMO and STON is inevitable after the connection of the two oxides. This will lead to a hole-depleted interface in the LCMO side, thus a growth in the dead layer, due to the depression of the double exchange by reduced hole density.

The oxygen content in LCMO/STON and LCMO/STO should be the same, considering that the two films have been simultaneously prepared. It therefore cannot be the origin of the different dead layers. The unexpected difference in dead layers cannot be ascribed to the difference in crystal quality of the LCMO films either. As shown by the XRD analysis, the LCMO films are clean single phase, with essentially the same lattice parameters on different substrates. The worse crystal orientation in LCMO/STON than that in LCMO/STO is expected to enhance the dead layer, if it has any effect on interface. This is different from what experimentally observed. Furthermore, AFM analysis shows a smooth surface morphology for the film and the absence of visible differences between LCMO/STO and LCMO/STON. This is an implication of similar growth mode for the films on different substrates.

LCMO/STON is different from LCMO/STO as far as the built-in electric field at its interface is concerned. This field can be as high as 10^7 V/m in magnitude, based on a simple estimation, and may have an effect on interface layer. In fact, the depression of resistivity by electric field has been widely observed in manganites. As reported by Asamitsu *et al.*[8] a drastic decrease in the resistivity of the $Pr_{0.7}Ca_{0.3}MnO_3$ single crystal can be produced by electric field, due to the field-induced melting of charge-ordered domains. Recently, Sun *et al.*[4] studied the influence of bias voltage on a ultrathin $La_{0.67}Sr_{0.33}MnO_3/LaAlO_3$ film (5 nm), and found an exponential decrease of the resistivity with applied voltage, $\rho \propto \exp(-\alpha V)$. A direct calculation shows a resistance reduction of three orders in magnitude as voltage increases from 10 to 300 V, the latter corresponds to an electric field of 10^6 V/m. Although it is generally difficult to distinguish electric field effect from current one, the delicate relation between resistivity and voltage observed by Sun *et al.*[4] seems to suggest the importance of electric field. These works demonstrate the dramatic effect of electric field on dead layer.

The possible scenario for the shrinkage of the dead layer in electric field is a challenging issue. As well established, the ferromagnetic/conductive and antiferromagnetic (paramagnetic)/insulating domains coexist near the interface of the manganite films.[3,4] The insulating domains will gain a polarization energy of $-\varepsilon_0\varepsilon_r \upsilon E^2$, whereas the conductive phase does not because of the absence of electric field,[9] where ε_0 is the permittivity of the vacuum, ε_r the relative permittivity of the insulating domains, E the electric field, and υ the domain volume. When partial domain becomes conductive, the electric field in the remaining parts will be enhanced for a fixed applied voltage. This implies the simultaneous occurrence of the decrease in domain volume and the growth in electric field. The resulting polarization energy will be decreased because of its square dependence on electric field and linear dependence on phase volume. A direct calculation shows that the change in the polarization energy, required by the insulating-conductive transition, is ~0.78 meV per unit cell in a field of 5×10^7 V/m, which is comparable to the energy destroying the charge ordering in the manganite (~0.8 meV for each Mn ion). This analysis indicates that part of the insulating domain may prefer to transit into the conductive one in the presence of electric field. Except for the mechanism discussed above, other effects may also exist. For example, a sufficient electrical field can affect the crystal and local symmetry of the ions and strongly influence the electronic state of Jahn–Teller centers. The stabilization of the conductive state in electric field could be a combined effect of various factors.

This work has been supported by the National Basic Research of China, the National Natural Science Foundation of China, the Knowledge Innovation Project of the Chinese Academy of Science, and the Beijing Municipal Nature Science Foundation.

[1] J. H. Park, E. Vescovo, H. J. Kim, C. Kwon, R. Ramesh, and T. Venkatesan, Phys. Rev. Lett. **81**, 1953 (1998).
[2] J. Z. Sun, D. W. Abraham, R. A. Rao, and C. B. Eom, Appl. Phys. Lett. **74**, 3017 (1999).
[3] M. Bibes, S. Valencia, L. Balcells, B. Martínez, J. Fontcuberta, M. Wojcik, S. Nadolski, and E. Jedryka, Phys. Rev. B **66**, 134416 (2002).
[4] Y. H. Sun, Y. G. Zhao, H. F. Tian, C. M. Xiong, B. T. Xie, M. H. Zhu, S. Park, W. Wu, J. Q. Li, and Q. Li, Phys. Rev. B **78**, 024412 (2008).
[5] J. R. Sun, C. M. Xiong, T. Y. Zhao, S. Y. Zhang, Y. F. Chen, and B. G. Shen, Appl. Phys. Lett. **84**, 1528 (2004).
[6] A. Sawa, T. Fujii, M. Kawasaki, and Y. Tokura, Appl. Phys. Lett. **86**, 112508 (2005).
[7] N. Nakagawa, M. Asai, Y. Mukunoki, T. Susaki, and H. Y. Hwang, Appl. Phys. Lett. **86**, 082504 (2005).
[8] A. Asamitsu, Y. Tomioka, H. Kuwahara, and Y. Tokura, Nature (London) **388**, 50 (1997).
[9] S. Dong, C. Zhu, Y. Wang, F. Yuan, K. F. Wang, and J.-M. Liu, J. Phys.: Condens. Matter **19**, 266202 (2007).

Author complimentary copy. Redistribution subject to AIP license or copyright, see http://apl.aip.org/apl/copyright.jsp